THE JOURNAL OF BIOLOGICAL CHEMISTRY VOL. 284, NO. 49, pp. 34296–34307, December 4, 2009

Mechanism for Amyloid Precursor-like Protein 2 Enhancement of Major Histocompatibility Complex Class I Molecule Degradation*[S]

Received for publication, July 1, 2009 Published, JBC Papers in Press, October 6, 2009, DOI 10.1074/jbc.M109.039727

Amit Tuli[‡§1], **Mahak Sharma**[‡2], **Haley L. Capek**[§3], **Naava Naslavsky**[‡], **Steve Caplan**[‡], **and Joyce C. Solheim**[‡§¶4]

From the [‡]*Department of Biochemistry and Molecular Biology,* [§]*Eppley Institute for Research in Cancer and Allied Diseases, and* [¶]*Department of Pathology and Microbiology, University of Nebraska Medical Center, Omaha, Nebraska 68198-6805*

Earlier studies have demonstrated interaction of the murine major histocompatibility complex (MHC) class I molecule K^d with amyloid precursor-like protein 2 (APLP2), a ubiquitously expressed member of the amyloid precursor protein family. Our current findings indicate that APLP2 is internalized in a clathrin-dependent manner, as shown by utilization of inhibitors of the clathrin pathway. Furthermore, we demonstrated that APLP2 and K^d bind at the cell surface and are internalized together. The APLP2 cytoplasmic tail contains two overlapping consensus motifs for binding to the adaptor protein-2 complex, and mutation of a tyrosine shared by both motifs severely impaired APLP2 internalization and ability to promote K^d endocytosis. Upon increased expression of wild type APLP2, K^d molecules were predominantly directed to the lysosomes rather than recycled to the plasma membrane. These findings suggest a model in which APLP2 binds K^d at the plasma membrane, facilitates uptake of K^d in a clathrin-dependent manner, and routes the endocytosed K^d to the lysosomal degradation pathway. Thus, APLP2 has a multistep trafficking function that influences the expression of major histocompatibility complex class I molecules at the plasma membrane.

The efficacy of the cellular immune response to intracellular pathogens and tumors is reliant on major histocompatibility complex (MHC)[5] class I molecules. MHC class I molecules present peptides, including peptides derived from pathogens and tumors, at the cell surface to cytotoxic T lymphocytes. Cytotoxic T lymphocytes have been selected during development for their ability to react to cells in the periphery expressing self MHC class I molecules bearing non-self peptides. The level of cell surface expression of MHC class I molecules on infected and malignant cells therefore dictates the extent to which the antigen-specific cytotoxic T lymphocytes can recognize, and subsequently lyse, abnormal cells. The cell surface expression of MHC class I molecules is controlled by the quantity and quality of MHC class I molecules that are assembled, and also by the rate at which MHC class I molecules depart from the plasma membrane.

Amyloid precursor-like protein 2 (APLP2) binds to the MHC class I molecule K^d in cells that express β2-microglobulin (1, 2). APLP2 regulates the level of folded K^d molecules at the cell surface: a reduction in APLP2 expression causes an elevation in the amount of folded K^d at the plasma membrane, and an increase in APLP2 expression results in a decline in folded K^d surface expression (3, 4). Higher APLP2 expression lowers the level of K^d at the plasma membrane by increasing the endocytosis, destabilization, and turnover of K^d molecules (4).

The family of proteins to which APLP2 belongs includes APL-1 in *Caenorhabditis elegans*, APPL in *Drosophila*, and three proteins in mammals: amyloid precursor protein (APP), amyloid precursor-like protein 1, and APLP2 (5, 6). APLP2 shares a high degree of sequence homology with APP, particularly at the C-terminal end. However, APP possesses a unique β-amyloid peptide domain that is not present within APLP2 (6).

APLP2 is a ubiquitously expressed protein with both a type I transmembrane form and a secreted form generated by proteolytic cleavage (7, 8). Functions for APLP2 have been shown in cell proliferation, cell adhesion, nerve growth, mitosis segregation, cell signaling, and transcriptional regulation (9–14). The APLP2 signaling/transcriptional function is mediated by a C-terminal cleavage product, which translocates to the nucleus (14, 15). By analogy to what is known from the study of the closely related protein APP, the cleavage of APLP2 that produces the free intracellular domain likely occurs after the arrival of the protein at the plasma membrane and may occur in endocytic compartments (16, 17).

Our recent studies have demonstrated that, in addition to K^d, APLP2 binds to other murine MHC class I molecules, with varied affinity (18). Furthermore, we have shown that APLP2 also binds to human MHC class I molecules, and that increased APLP2 expression causes down-regulation of human MHC class I molecules at the plasma membrane (19). The impact of

* This work was supported, in whole or in part, by National Institutes of Health Grants GM57428 (to J. C. S.) and GM74876 (to S. C.), a Nebraska Cancer and Smoking Disease Research Program grant, and an Eppley Cancer Center Pediatric Cancer Research grant (to J. C. S.).

[S] The on-line version of this article (available at http://www.jbc.org) contains supplemental Figs. S1 and S2.

[1] Supported by a University of Nebraska Medical Center Graduate Studies Fellowship.

[2] Supported by University of Nebraska Medical Center Graduate Studies, Nebraska Center for Cellular Signaling, and American Heart Association Predoctoral Fellowships.

[3] Supported by a Structural Biology and Biophysics Fellowship.

[4] To whom correspondence should be addressed: Eppley Institute for Research in Cancer and Allied Diseases, University of Nebraska Medical Center, 986805 Nebraska Medical Center, Omaha, NE 68198-6805. Tel.: 402-559-4539; Fax: 402-559-4651; E-mail: jsolheim@unmc.edu.

[5] The abbreviations used are: MHC, major histocompatibility complex; APLP2, amyloid precursor-like protein 2; APP, amyloid precursor protein; CHAPS, 3-[(3-cholamidopropyl)dimethylammonio]-1-propanesulfonate; EHD, Eps15 homology domain; Ab, antibody; EGFP, enhanced green fluorescent protein; PBS, phosphate-buffered saline; AP-2, adaptor protein-2.

APLP2 on cell surface expression of the MHC class I molecule, and the site of APLP2/MHC class I co-localization within the cell, depends on the specific MHC class I allotype (18). The polymorphic $\alpha1/\alpha2$ domain and conserved ($\alpha3$/transmembrane/cytoplasmic) regions of the MHC class I molecule are involved in interaction with APLP2 (18).

Although our previous studies demonstrated that APLP2 is bound to the endocytosed K^d molecule, the specific location where the binding occurs was not identified (4). In the present study, we established that APLP2 binds K^d at the cell surface before these two proteins internalize into the same endocytic vesicles. Our results demonstrated that APLP2 is principally endocytosed by a clathrin-mediated process, because a dominant-negative dynamin II K44A mutant and the C-terminal portion of AP180, both of which inhibit clathrin-dependent endocytosis (20, 21), blocked APLP2 internalization. Furthermore, clathrin-mediated endocytosis of APLP2 was required for APLP2 to promote K^d endocytosis. The APLP2 cytoplasmic tail contains overlapping tyrosine-based NP*X*Y and Y*XXØ* motifs for adaptor protein-2 (AP-2) binding (22, 23), and we demonstrated that mutation of the tyrosine included in both motifs impaired internalization of APLP2, indicating the importance of this sequence in APLP2 endocytosis. APLP2 mutated at this cytoplasmic domain tyrosine residue, in contrast to wild type APLP2, was unable to facilitate the endocytosis of K^d. Cells expressing a high level of APLP2 were noted to have relatively few internalized K^d molecules recycling to the plasma membrane, and delivery of K^d to the lysosomes in these cells was shown by inhibition of lysosomal function with ammonium chloride. Our findings indicate that APLP2 is endocytosed by a clathrin-dependent mechanism, and that APLP2 utilizes clathrin-mediated endocytosis to increase the internalization of K^d bound by APLP2 at the cell surface. Furthermore, our data demonstrate that APLP2 directs K^d molecules to lysosomes and the K^d molecules are degraded rather than recycled to the cell surface.

EXPERIMENTAL PROCEDURES

Antibodies (Abs)—Monoclonal Ab 34-1-2 recognizes the $\alpha1/\alpha2$ domain of K^d (24). The 64-3-7 monoclonal Ab can detect open, peptide-free L^d (24, 25) and can also detect open forms of other MHC class I heavy chains, such as K^d, into which the 64-3-7 epitope has been introduced, and addition of the 64-3-7 epitope does not impair peptide presentation, trafficking, or surface expression of K^d or other MHC class I molecules (26–29). The 34-1-2 and 64-3-7 Abs were donated by Dr. T. Hansen (Washington University, St. Louis, MO). The Ab used for APLP2 detection was made against full-length APLP2 (Calbiochem). Rabbit anti-FLAG Ab was obtained from Cell Signaling, mouse anti-FLAG Ab was purchased from Sigma, and fluorescein isothiocyanate-conjugated goat anti-FLAG Ab was obtained from AbD Serotec. The rabbit anti-LAMP1 Ab was from Novus Biologicals. All Alexa Fluor secondary Abs used for immunofluorescence were purchased from Molecular Probes.

Cell Lines—Cells were cultured in RPMI 1640 medium (Invitrogen) containing glutamine, pyruvate, penicillin/streptomycin, and 15% fetal bovine serum. The HeLa cells were given by Dr. W. Maury (University of Iowa, Iowa City, IA). The HeLa cells were transfected with a cDNA for K^d bearing the 64-3-7 epitope (etK^d) (26) in the pIRIS.puro2 vector (BD Biosciences Clontech) and were selected with puromycin. For some experiments, a C-terminal FLAG-tagged APLP2 cDNA in pCMVTag4A (Stratagene) was transiently transfected into HeLa-etK^d to make HeLa-etK^d cells that expressed APLP2 at higher levels. GFP-tagged Rab5 and Rab5Q79L cDNAs (30) in the EGFP vector (Clontech), kindly donated by Dr. R. Lodge, were transiently transfected into HeLa-etK^d cells for some experiments. The GFP-dynamin II K44A mutant cDNA (20) in a pEGFP N1 vector (Clontech), used in transient transfections, was a gift from M. McNiven (Mayo Clinic, Rochester, MN). The FLAG-tagged C-terminal fragment of AP180 in the pFLAG-CMV2 vector that was used for transient transfections was contributed by Dr. J. Donaldson and Dr. L. Greene (National Institutes of Health, NICHD, Bethesda, MD). All transient transfections were done with Effectene (Qiagen), using 1 μg of DNA per 0.5×10^6 cells.

Immunoprecipitations and Western Blots—For immunoprecipitation and Western blotting, variations of published protocols (31) were used. For washes prior to lysis of cells, PBS containing 20 mM iodoacetamide (Sigma) was used, and the washes were done three times. Cells were lysed in CHAPS lysis buffer, which was 1% CHAPS (Roche Applied Science) in Tris-buffered saline (pH 7.4) with freshly added 0.2 mM phenylmethylsulfonyl fluoride and 20 mM iodoacetamide. For some experimental samples, the lysis buffer also contained a freshly added, saturating quantity of monoclonal Ab. For all samples, after 45 min with intermittent gentle mixing, the samples were centrifuged and the Protein A-Sepharose beads were washed in 0.1% CHAPS, 20 mM iodoacetamide in TBS (pH 7.4) four times and boiled in 0.125 M Tris (pH 6.8), 2% SDS, 12% glycerol, 0.02% bromphenol blue to elute the proteins. The eluates were electrophoresed on 4–20% Tris glycine acrylamide gels (Invitrogen).

For Western blots, the proteins were transferred to Immobilon-P blotting membranes (Millipore). After blocking in reconstituted dry milk overnight at room temperature, the blots were incubated in a dilution of Ab for 2 h at room temperature, washed 3 times for 15 min with 0.05% Tween 20/PBS, and incubated 1 h in diluted biotin-conjugated goat anti-mouse or anti-rabbit IgG (Caltag Laboratories). Following 3 washes in 0.05% Tween 20/PBS, the blots were incubated 1 h in diluted streptavidin-conjugated horseradish peroxidase (Zymed Laboratories Inc.). The blots were washed 3 times for 15 min with 0.3% Tween 20/PBS and then treated with enhanced chemiluminescence Western blot reagents (GE Healthcare). The blots were exposed to Kodak Bio-Max film (Eastman Kodak Co., Rochester, NY) for visualization of the bands.

Immunoprecipitation and Western blotting were done to confirm the binding of the APLP2-Y755A-FLAG, APLP2-Y721A-FLAG, and APLP2-Y721A/Y755A-FLAG mutants to K^d. For these experiments, the membranes were incubated in a dilution of Ab for 2 h at room temperature, washed 3 times with 0.05% Tween 20/PBS, and incubated for 1 h at room temperature in diluted horseradish peroxidase-conjugated goat anti-mouse Ab (Jackson ImmunoResearch). After three washes in 0.1% Tween 20/PBS, the membranes were treated with

enhanced chemiluminescence reagents and exposed to film as described above.

Immunofluorescence Analysis—For immunofluorescence analysis, cells were grown on glass coverslips. For some experiments, cells were incubated at 37 °C to allow internalization of proteins and Abs bound to them, and the remaining Abs still bound at the cell surface (not internalized) were removed by incubation in stripping buffer (0.5% acetic acid, 500 mM NaCl) for 90 s. The stripping step ensured that the subsequent immunofluorescence analysis would reveal only proteins that had been internalized. Cells were fixed with a solution of 4% (v/v) paraformaldehyde in PBS for 10 min. Ab incubations were done in staining solution (0.2% (w/v) saponin, 0.5% (w/v) bovine serum albumin/PBS) for 30 min at room temperature, unless otherwise specified. As a control for clathrin-mediated endocytosis, HeLa-etK^d cells transfected with a cDNA for GFP-tagged dynamin II K44A or the FLAG-tagged AP180 C-terminal fragment were pulsed with fluorochrome-labeled transferrin (Tf-568 from Molecular Probes) for 5 min at 37 °C.

In all immunofluorescence analysis experiments, PBS washes were 5 min at room temperature, and immediately prior to mounting for image analysis the cells were washed 3 times in PBS. All images were obtained with a Zeiss LSM 5 Pascal confocal microscope. A ×63 1.4 numerical aperture lens with appropriate filters was used. For some experiments, ImageJ software (rsb.info.nih.gov) was used to measure the fluorescence of the Ab-labeled internalized K^d molecules. The mean fluorescence intensity was calculated with the histogram tool in ImageJ, using data from >80 cells of each type within a total of >10 images acquired with the same optical settings.

RESULTS

APLP2 and K^d Bind at the Plasma Membrane and Are Internalized Together—Previous studies from our laboratories showed that APLP2 co-localized in endosomes with K^d internalized from the cell surface and that APLP2 could be co-immunoprecipitated with internalized K^d (4). To determine whether the interaction between APLP2 and K^d occurs at the cell surface, K^d molecules at the surface of HeLa-etK^d cells were labeled with the 34-1-2 Ab on ice for 20 min, and then the cells were lysed and Ab complexes isolated with Protein A-Sepharose. The complexes were electrophoresed, blotted, and probed with Abs to identify the K^d heavy chain (Fig. 1*A*, *top panel*) or APLP2 (Fig. 1*A*, *bottom panel*). As controls, the same surface labeling procedure was performed using HeLa cells, and immunoprecipitations were done with Ab 34-1-2 using lysates of HeLa-etK^d and HeLa cells that had not been surface labeled (Fig. 1*A*). From the lysates of HeLa-etK^d cells labeled at the cell surface with 34-1-2 and maintained on ice to prevent internalization, APLP2 was co-immunoprecipitated with K^d (Fig. 1*A*, *bottom panel*, *lane 5*). This approach specifically immunoprecipitated cell surface K^d, as confirmed by the presence of only the high molecular weight (presumably glycosylated) K^d in *lane 5* (Fig. 1*A*, *top panel*).

As mentioned above, earlier studies from our laboratories showed that APLP2 and internalized K^d co-localized in endosomes; however, these studies had not ascertained whether any of these APLP2 molecules were also internalized from the cell surface. To determine whether APLP2 co-localized with K^d after both molecules were internalized from the cell surface, co-localization analysis was performed. HeLa-etK^d cells were incubated with 34-1-2 and anti-APLP2 Abs for 12 min and the remaining Abs at the cell surface were removed. Cells were fixed, permeabilized, and stained with fluorescently labeled secondary Ab. As shown by the representative *z*-section in Fig. 1*B*, the K^d and APLP2 molecules internalized from the cell surface were co-localized in the same vesicular compartments. To analyze whether the vesicles in which the internalized APLP2 and K^d co-localized were endosomes, HeLa-etK^d cells were transiently transfected with either GFP-Rab5 (Fig. 1*C*) or GFP-Rab5Q79L (Fig. 1*D*), and then surface labeled with Abs for K^d and APLP2. Rab5 is an endosomal marker, and Rab5Q79L is a dominant-active Rab5 mutant that causes enlargement of early endosomes accessible to internalized proteins (30), thereby facilitating endosomal compartment identification by confocal microscopy. The internalization of Ab-labeled K^d and APLP2 molecules was induced by incubating the cells at 37 °C for 15 min. The remaining Ab at the cell surface was removed by acid washing, and the cells were permeabilized and stained with secondary Ab. APLP2 and K^d, both endocytosed from the cell surface, were visualized within the same Rab5$^+$ endosomal vesicles.

Internalization of APLP2 by a Clathrin-dependent Mechanism and K^d by a Clathrin-independent Mechanism—In an earlier study, we showed that increased expression of APLP2 reduces cell surface K^d levels (4). As a step toward understanding the mechanisms by which elevated APLP2 expression increases the endocytosis of K^d molecules, we assessed the means by which APLP2 itself is endocytosed. HeLa-etK^d cells were transiently transfected with a dominant-negative dynamin II mutant, K44A, or with the C terminus of AP180. Both dynamin II K44A and the C-terminal portion of AP180 have been shown previously to inhibit clathrin-dependent endocytosis (20, 21). To determine whether the dynamin II dominant-negative mutant or the C terminus of AP180 could down-regulate endocytosis of APLP2, each was transiently transfected into HeLa-etK^d cells, and confocal microscopy was used to assess APLP2 internalization.

As shown in Fig. 2*A*, the expression of GFP-dynamin II K44A hindered the internalization of APLP2, indicating that APLP2 is endocytosed by a clathrin-dependent mechanism. Expression of GFP-dynamin II K44A also blocked the uptake of transferrin (included as a positive control), which is known to be a clathrin-mediated process (data not shown). The presence of the C-terminal fragment of AP180-FLAG also prevented APLP2 and transferrin endocytosis (Fig. 2*B* and data not shown), consistent with our results using the GFP-dynamin II mutant. (As a control, the level of surface staining of APLP2, without allowing APLP2 internalization, was assessed for comparison (supplemental Fig. S1).) In contrast, the endocytosis of K^d was not inhibited by either GFP-dynamin II K44A or the C-terminal portion of AP180-FLAG (Fig. 2, *C* and *D*), suggesting K^d is predominantly endocytosed in HeLa-etK^d cells by a clathrin-independent pathway.

Internalization of APLP2 by a Clathrin-mediated Endocytic Mechanism Was Necessary for APLP2 to Facilitate K^d

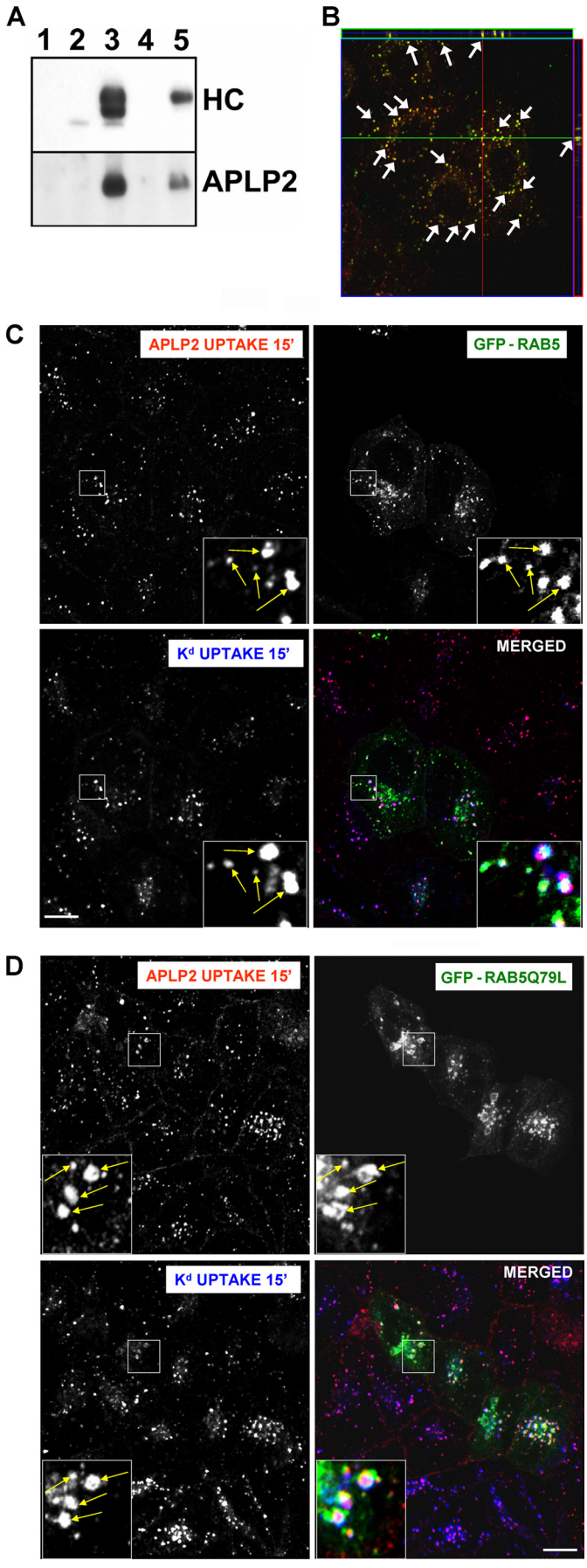

Endocytosis—By binding to K^d, APLP2 may recruit K^d into the clathrin-mediated endocytic pathway as APLP2 itself is internalized. If so, then the tendency of APLP2 to increase K^d endocytosis would depend upon the ability of APLP2 to be endocytosed. As a control, we incubated HeLa-K^d cells that were transiently transfected with APLP2-FLAG with the 34-1-2 Ab to label the cell surface K^d molecules and warmed the cells at 37 °C to cause the K^d molecules to be internalized. The remaining Abs at the surface were stripped off by an acid wash (with stripping buffer), and the cells were fixed and stained with anti-FLAG Ab. As expected from our previous study (4), cells that expressed APLP2-FLAG contained more endocytosed K^d, relative to cells not expressing APLP2-FLAG (Fig. 3*A*). To determine whether APLP2 must be endocytosed for it to increase K^d endocytosis, HeLa-etK^d cells were transiently transfected with both APLP2-FLAG and the GFP-tagged dynamin II K44A dominant-negative mutant. The cells were pulsed with the 34-1-2 Ab to label the cell surface K^d molecules and the K^d molecules were allowed to internalize, then the remaining Abs at the surface were removed, and the cells were fixed and stained with anti-FLAG Ab. After washing, the cells were incubated with secondary Abs to identify the APLP2-FLAG and K^d molecules (Fig. 3*B*). In contrast to the control results showing significantly higher numbers of K^d molecules endocytosed in cells expressing APLP2-FLAG (in cells not transfected with GFP-dynamin II K44A) (Fig. 3*C*), the results displayed in Fig. 3*D* demonstrated that the expression of GFP-dynamin II K44A prevented enhancement of K^d internalization by APLP2, as there was no difference in the quantity of K^d molecules endocytosed in cells co-expressing both transfected APLP2-FLAG and GFP-dynamin II K44A, compared with cells expressing neither. These data suggest that overexpression of APLP2 causes enhanced endocytosis of K^d through the clathrin pathway but expression of the dynamin II K44A mutant abolishes this effect.

FIGURE 1. **APLP2 bound K^d at the cell surface and they internalized together into common Rab5$^+$ early endosomes.** *A*, K^d was demonstrated to bind APLP2 at the cell surface. *Lane 1*, HeLa-etK^d cells were lysed and Protein A-Sepharose beads were added to the centrifuged lysate supernatant. *Lanes 2* and *3*, immunoprecipitations were performed with anti-K^d Ab 34-1-2 on HeLa and HeLa-etK^d lysates. *Lanes 4* and *5*, HeLa and HeLa-etK^d cells were incubated with Ab 34-1-2 on ice for 20 min, the cells were lysed and centrifuged, and Protein A-Sepharose beads were added to the supernatant. All samples were Western blotted with the 64-3-7 Ab to detect the etK^d heavy chain (*HC*) or with anti-APLP2 Ab. *B*, K^d and APLP2 were identified as co-localized within vesicular compartments. Cell surface K^d and APLP2 molecules were labeled with 34-1-2 Ab and anti-APLP2 Ab, respectively, for 12 min at 37 °C to allow internalization of labeled proteins with the bound Abs, and any remaining Abs at the surface were removed. Cells were then fixed and stained with Alexa Fluor 568 goat anti-mouse Ab and Alexa Fluor 488 goat anti-rabbit Ab. Serial *z*-section images were acquired for HeLa-etK^d cells, and the *arrows* point to common membrane structures on a representative *z*-section micrograph (obtained from six slices imaged at 0.4-μm intervals). *Red*, K^d; *green*, = APLP2; *yellow*, co-localized K^d and APLP2. *C* and *D*, cell surface K^d and APLP2 were internalized into the same endocytic vesicles. HeLa-etK^d cells were transfected with either (*C*) GFP-Rab5 or (*D*) GFP-Rab5Q79L for 24 h, then pulsed with anti-K^d Ab 34-1-2 and anti-APLP2 Ab and incubated in complete medium for 15 min at 37 °C. Following the incubation, non-internalized Abs were removed. The cells were fixed, permeabilized, and stained with Alexa Fluor 568 goat anti-rabbit and Alexa Fluor 405 goat anti-mouse Abs. *Red*, APLP2; *green*, GFP-Rab5 or GFP-Rab5Q79L; *blue*, K^d; *white*, co-localized APLP2, K^d, and GFP-Rab5 or GFP-Rab5Q79L. *Bar*, 10 μm. The *insets* show a higher magnification of areas within the larger boxes, and the *arrows* point to representative endosomes with co-localized APLP2 and K^d.

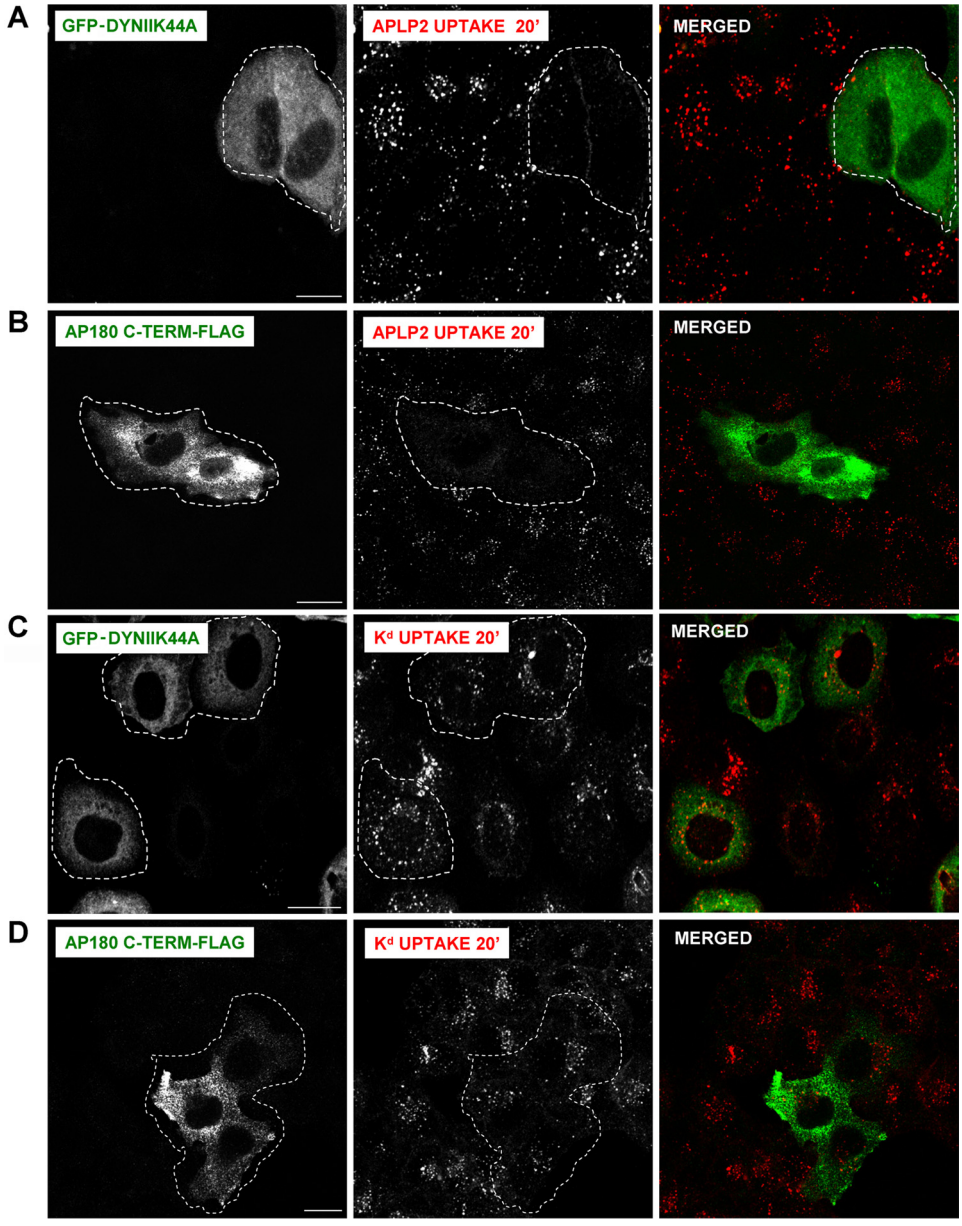

FIGURE 2. **APLP2 was demonstrated to be endocytosed by a clathrin-mediated mechanism, but K^d was shown to be endocytosed principally by a clathrin-independent mechanism.** HeLa-etK^d cells were transfected for 24 h with a cDNA encoding (*A* and *C*) GFP-tagged dynamin II K44A or (*B* and *D*) C-terminal fragment of AP180-FLAG. Cells were pulsed with (*A* and *B*) anti-APLP2 or (*C* and *D*) anti-K^d Ab at 37 °C for 20 min to allow Ab binding and internalization, and then the cells were stripped of non-internalized surface-bound Ab and fixed. Cells in *B* and *D* were stained with anti-FLAG Ab for 1 h in saponin-containing staining solution to visualize the AP180 C-terminal fragment (using rabbit anti-FLAG Ab if 34-1-2 Ab had been used for the pulse, or mouse anti-FLAG Ab if anti-APLP2 Ab had been used for the pulse). The cells transfected with GFP-dynamin II K44A were incubated with Alexa Fluor 568 goat anti-mouse secondary Ab to visualize internalized K^d or with Alexa Fluor 568 goat anti-rabbit Ab to reveal internalized APLP2. For AP180-FLAG C terminus transfectants, the cells were incubated with Alexa Fluor 568 goat anti-mouse Ab and Alexa Fluor 488 goat anti-rabbit Ab if a 34-1-2 Ab pulse had been done, or with Alexa Fluor 488 goat anti-mouse Ab and Alexa Fluor 568 goat anti-rabbit Ab if an anti-APLP2 Ab pulse had been done. *A* and *B*, *red*, APLP2; *C* and *D*, *red*, K^d; *A* and *C*, *green*, GFP-dynamin II K44A; *B* and *D*, *green*, AP180 C terminus-FLAG. *Bar*, 10 μm. Cells shown *bordered with white* are transfected with GFP-dynamin II K44A or AP180 C terminus-FLAG.

APLP2 cytoplasmic tail. We mutated the tyrosine residue in each of these sequences to an alanine (singly or together), and generated constructs with these APLP2 mutants (Y755A, Y721A, or Y721A/Y755A) bearing a C-terminal attached FLAG tag.

To verify that the tyrosine mutations did not disrupt binding of APLP2 to K^d, HeLa-etK^d cells were transiently transfected with vector only, wild type APLP2-FLAG, or each of the three mutant APLP2-FLAG constructs. The cells were lysed and immunoprecipitations were performed with anti-FLAG Ab to isolate FLAG-tagged proteins. The immunoprecipitates were Western blotted with anti-APLP2 Ab to confirm the quality of the immunoprecipitations or with 64-3-7 to detect the presence of co-immunoprecipitated K^d. Results demonstrating K^d binding to APLP2-Y755A-FLAG are shown in Fig. 4*A*, and similar results indicating K^d association were obtained for APLP2-Y721A-FLAG and APLP2-Y721A/Y755A-FLAG (data not shown).

For assessment of the effect of the Y755A mutation on APLP2 endocytosis and on the ability of APLP2 to facilitate K^d endocytosis, cells transfected with either wild type APLP2-FLAG or APLP2-Y755A-FLAG were incubated with anti-APLP2 Ab at 37 °C to allow APLP2 internalization. Cell surface APLP2 was taken up normally in cells transfected with APLP2-FLAG (Fig. 4*B*, *left panel*). However, mutation of the Tyr-755 residue to alanine in APLP2 inhibited the internalization of cell surface APLP2 (Fig. 4*B*, *right panel*), indicating that Tyr-755 is required for APLP2 to internalize. In addition, it appears from these data that the expression of APLP2-Y755A-FLAG also likely inhibited the uptake of wild type, endogenous APLP2 (Fig. 4*B*, *right panel*). (Surface staining of APLP2, without warming the cells to permit internalization, was monitored as a control (supplemental Fig. S2).) We also found that the impairment of APLP2 endocytosis was very similar for APLP2-Y721A/Y755A-FLAG as compared with APLP2-Y755A-FLAG (data not shown). In contrast, we found no difference in APLP2 endocytosis between APLP2-Y721A-

A Tyrosine in the APLP2 C Terminus Was Required for the Effect of APLP2 on K^d Internalization—NP*X*Y and Y*XXØ* sequence motifs present in other proteins bind to the AP-2 complex (21, 22). These two endocytic motifs (NP*X*Y and Y*XXØ*) overlap within the amino acid sequence NPTYKYL of the APLP2 cytoplasmic tail. An additional Y*XXØ* putative endocytic motif (in the sequence YGTI) is also present in the

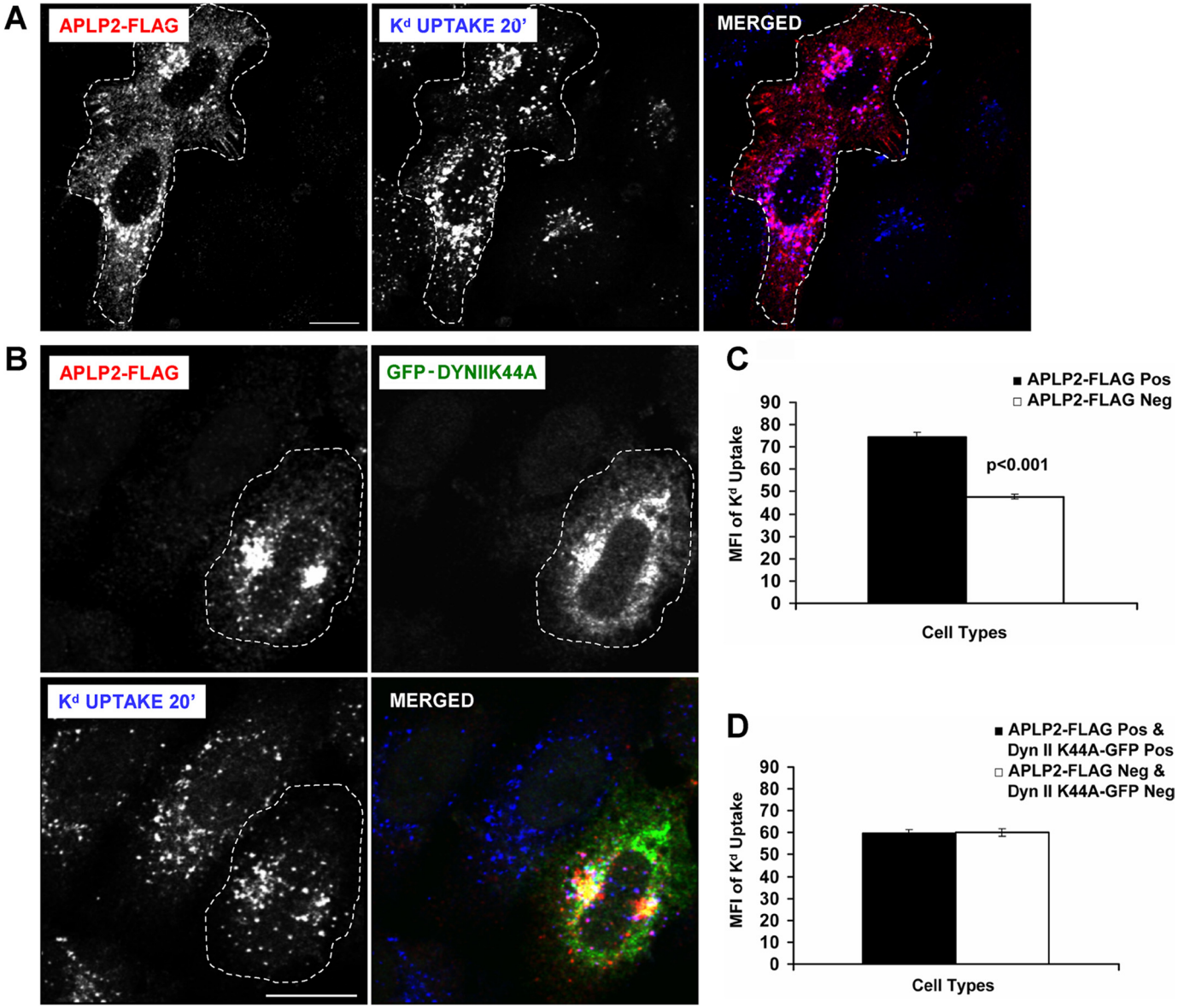

FIGURE 3. **Blocking clathrin-mediated endocytosis by expression of dynamin II K44A prevented APLP2 from increasing K^d endocytosis.** *A*, HeLa-etK^d cells transfected transiently with APLP2-FLAG (but not GFP-dynamin II K44A) for 24 h were pulsed with 34-1-2 Ab for 20 min in complete medium. At the end of the pulse period, non-internalized cell surface-bound Abs were removed. After fixation, the cells were stained with rabbit anti-FLAG Ab for 1 h. The cells were incubated with Alexa Fluor 568 goat anti-rabbit Ab to identify APLP2-FLAG and Alexa Fluor 405 goat anti-mouse Ab to identify 34-1-2-bound K^d. *Red*, APLP2-FLAG; *blue*, K^d. *Bar* corresponds to 10 μm. Cells expressing APLP2-FLAG are *encircled* with a *dashed white line*. *B*, the same procedure described in *A* was followed except that the HeLa-etK^d cells were co-transfected transiently with both APLP2-FLAG and GFP-dynamin II K44A for 24 h. *Red*, APLP2-FLAG; *green*, GFP-dynamin II K44A; *blue*, K^d. *Bar* corresponds to 10 μm. Cells co-expressing APLP2-FLAG and GFP-dynamin II K44A are *encircled with a dashed white line*. *C*, ImageJ software was used to measure the internalized K^d fluorescence for >80 cells transfected with APLP2-FLAG *versus* no APLP2-FLAG. Note that in this control no cells were transfected with GFP-dynamin II K44A, and APLP2-FLAG was able to increase K^d endocytosis. *D*, Image J software was used to measure the internalized K^d fluorescence for >80 cells expressing both APLP2-FLAG and GFP-dynamin II K44A, as well as >80 cells expressing neither protein. In this case, some of the cells expressed GFP-dynamin II K44A, and APLP2-FLAG was not able to increase K^d endocytosis if GFP-dynamin II K44A was also expressed in the same cell. *C* and *D*, mean fluorescence intensities and mean ± S.E. were calculated, and *p* values were determined by Student's paired *t* test: *C*, $p < 0.001$; *D*, $p = 0.81$.

FLAG and wild type APLP2-FLAG (data not shown), indicating that the Tyr-721 position does not contribute to APLP2 internalization.

The APLP2 sequence NPTYKYL contains overlapping NP*X*Y and Y*XX*Ø motifs, with Tyr-755 at the intersection of the two motifs. In studies on other proteins, it has been shown that both of these motifs can interact with AP μ subunits; however, only the NP*X*Y motif has been demonstrated to interact with Dab2 (23, 32–34). We have found that transfection with AP-2 μ2 small interfering RNA largely abrogates internalization of APLP2, suggesting that APLP2 endocytosis is mediated by the AP-2 complex. In contrast, we found that Dab2 small interfering RNA transfection caused little decrease in APLP2 endocytosis, indicating that Dab2-mediated clathrin-dependent endocytosis is a minor pathway for APLP2 internalization. However, transfection with both small interfering RNA for the AP-2 μ2 subunit and Dab2 resulted in greater inhibition of APLP2 endocytosis

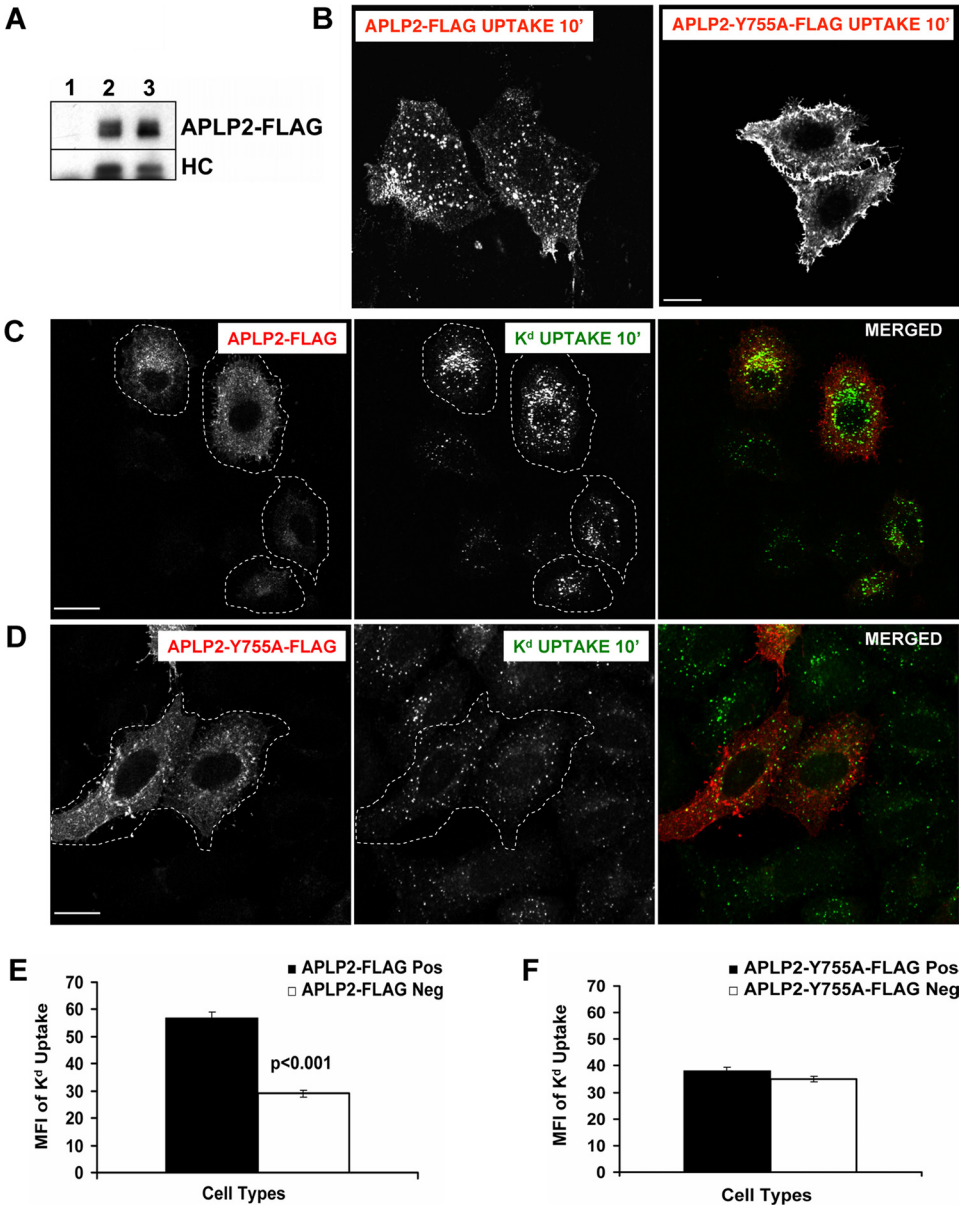

FIGURE 4. **The tyrosine residue at position 755 in the APLP2 C terminus was found to be required for APLP2 to facilitate K^d endocytosis.** *A*, APLP2-Y755A-FLAG was demonstrated to bind K^d. Lysates of HeLa-etK^d cells (*lane 1*), HeLa-etK^d cells (*lane 2*) transfected for 24 h with APLP2-FLAG, or HeLa-etK^d cells (*lane 3*) transfected for 24 h with APLP2-Y755A-FLAG were immunoprecipitated with the anti-FLAG Ab. The immunoprecipitates were Western blotted with anti-APLP2 Ab to detect the immunoprecipitated APLP2-FLAG or APLP2-Y755A-FLAG or with the 64-3-7 monoclonal Ab to detect the etK^d heavy chain (*HC*). *B–D*, HeLa-etK^d cells transfected with APLP2-FLAG or APLP2-Y755A-FLAG for 24 h were pulsed with anti-APLP2 rabbit Ab (*B*) or with anti-K^d (34-1-2) Ab (*C* and *D*) for 10 min at 37 °C. *C* and *D*, after the pulse period, non-internalized cell surface-bound Abs were removed. *B–D*, the cells were fixed, incubated for 1 h with mouse anti-FLAG (*B*) or rabbit anti-FLAG Ab (*C* and *D*) to identify transfected cells, and stained with fluorochrome-conjugated secondary Abs. *Bar*, 10 μm. *B*, secondary Ab Alexa Fluor 488 (goat anti-mouse Ab) staining was done to identify APLP2-FLAG- or APLP2-Y755A-FLAG-transfected cells, and the image shows the Alexa Fluor 568 (goat anti-rabbit) staining to visualize any internalized wild type APLP2-FLAG, APLP2-Y755A-FLAG, or wild type APLP2 (non-FLAG-tagged) molecules. *C* and *D*, Alexa Fluor 568 (goat anti-rabbit Ab) staining was used to identify APLP2-Y755A-FLAG or APLP2-FLAG, and Alexa Fluor 488 (goat anti-mouse Ab) was used to identify internalized, 34-1-2-bound K^d. *Red*, APLP2-FLAG; *green*, K^d; *yellow*, co-localized APLP2-FLAG and K^d. Cells *encircled with white dashed lines* are transfected with APLP2-FLAG (*C*) or APLP2-Y755A-FLAG (*D*). *E*, ImageJ software was used to measure the fluorescence of the internalized K^d for >80 cells expressing APLP2-FLAG and >80 cells not expressing APLP2-FLAG. *F*, Image J software was used to measure the internalized K^d fluorescence for >80 cells expressing APLP2-Y755A-FLAG and >80 cells not expressing APLP2-Y755A-FLAG. *E* and *F*, mean fluorescence intensities and mean ± S.E. were calculated, and *p* values were determined by the Student's paired *t* test.

than either small interfering RNA alone, evidently due to blockage of both major and minor pathways of APLP2 internalization (data not shown). Overall, these findings are consistent with a major role for the Y*XXØ* motif and a more minor role for the NP*X*Y motif in APLP2 endocytosis.

When HeLa-etK^d cells expressing either APLP2-Y755A-FLAG or wild type APLP2-FLAG were labeled with anti-K^d Ab and the cells were incubated at 37 °C to induce K^d endocytosis, the FLAG-tagged APLP2 Y755A, in contrast to wild-type APLP2-FLAG, did not promote K^d endocytosis (Fig. 4, *C* and *D*). A statistically significant difference was found between the number of endocytosed K^d molecules in cells expressing APLP2-FLAG *versus* no APLP2-FLAG (Fig. 4*E*), but not between the number of internalized K^d molecules in cells with APLP2-Y755A-FLAG *versus* no APLP2-Y755A-FLAG (Fig. 4*F*). Therefore, the Tyr-755-mediated endocytosis of APLP2 is necessary for APLP2 to facilitate K^d endocytosis.

Elevated Expression of APLP2 Increased Shuttling of K^d to the Lysosomes Rather Than Back to the Plasma Membrane—Our findings raised the question of what was the fate of the K^d molecules that were shuttled to the clathrin-mediated endocytosis pathway by APLP2. For investigation of the subcellular itinerary of K^d in cells that expressed lower and higher levels of APLP2, HeLa-etK^d cells were transiently transfected with APLP2-FLAG, pulsed with anti-K^d Ab 34-1-2 and warmed to 37 °C, stripped of non-internalized Abs by acid wash, and either directly fixed (Fig. 5*A*) or first chased for 2 h and then fixed (Fig. 5*B*). Staining with anti-FLAG Ab and comparison of cells within the same fields that were not transfected *versus* transfected with APLP2 revealed that K^d recycling after 2 h was decreased in cells expressing a higher level of APLP2 (Fig. 5*B*). In cells that were not transfected with APLP2-FLAG, by 2 h of chase most of the internalized 34-1-2-bound K^d molecules had recycled back to the plasma membrane (indicated by *arrows*), although a few remained in vesicles within the cells (Fig. 5, *B* and *C*). However, in cells transfected with APLP2-FLAG (examples are shown encircled with a white

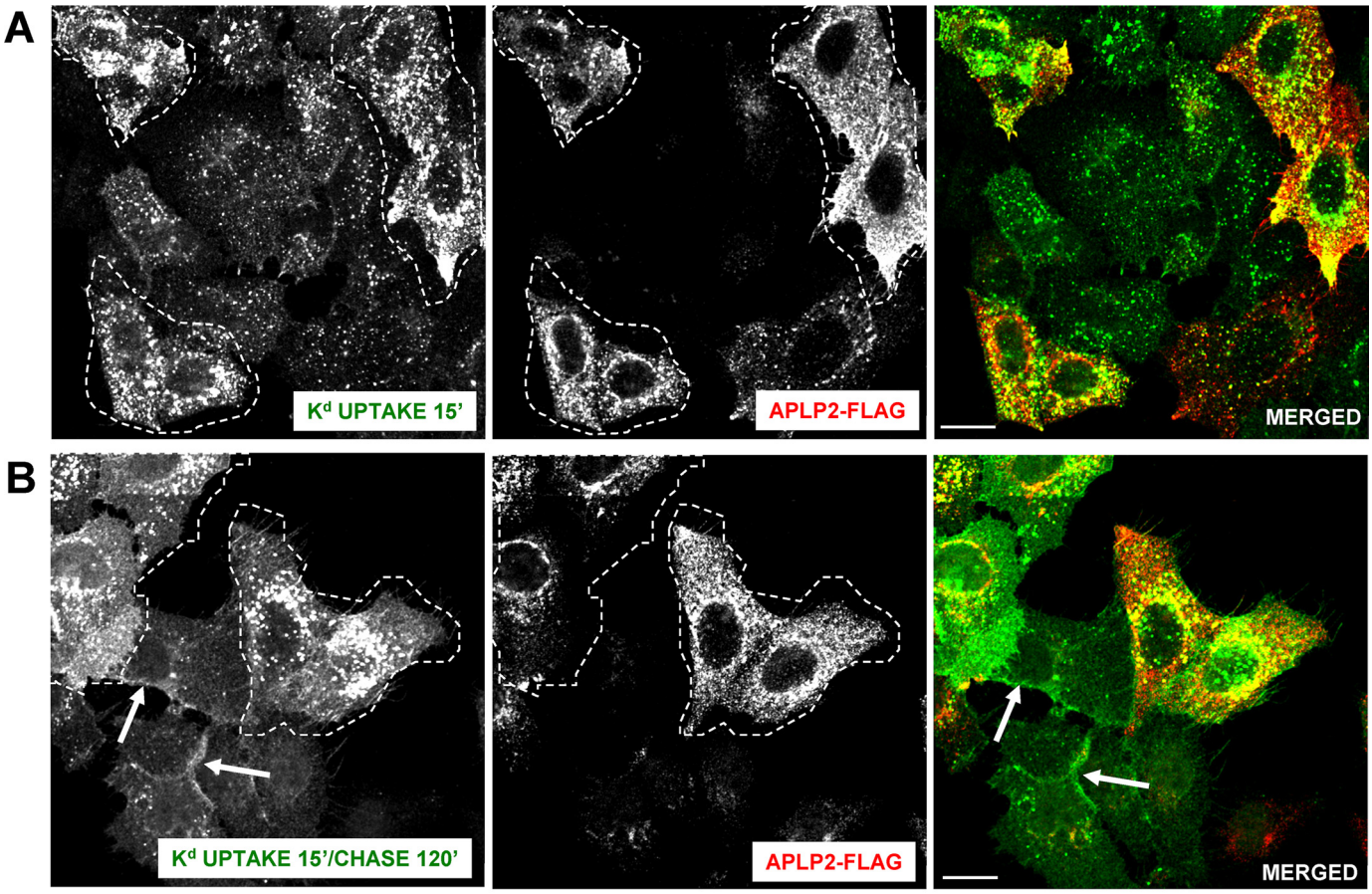

FIGURE 5. **K^d recycling was reduced in cells expressing an increased level of APLP2.** *A*, HeLa-etK^d cells transfected with APLP2-FLAG for 24 h were pulsed for 15 min at 37 °C with anti-K^d Ab 34-1-2. After the pulse period, non-internalized cell surface-bound Abs were removed. The cells were fixed, incubated for 1 h with rabbit anti-FLAG Ab, and stained with Alexa Fluor 488 goat anti-mouse Ab and Alexa Fluor 568 goat anti-rabbit Ab. *B*, the same procedure described in *A* was followed except that the cells were transferred to complete medium for 2 h after cell surface-bound Abs were removed with stripping buffer, and at the end of the 2-h chase period the cells were fixed and stained. *Arrows* indicate internalized K^d that had recycled to the plasma membrane (*A* and *B*). *Red*, APLP2-FLAG; *green*, K^d; *yellow*, co-localized APLP2-FLAG and K^d. *Bar*, 10 μm. Cells *outlined with white boundaries* are transfected with APLP2-FLAG. *C*, comparison of intracellular K^d in HeLa-etK^d cells transfected with APLP2 *versus* untransfected cells in the same experiment. Quantification of mean fluorescence intensity of the stained intracellular K^d was done with ImageJ software using data from >70 cells in each group. The graph shows the mean fluorescence intensity values, and the *error bars* on the graph indicate the mean ± S.E. for each sample set.

boundary), a majority of the 34-1-2-bound K^d molecules were still localized to the cell interior at 2 h (Fig. 5, *B* and *C*). These data suggest that APLP2 not only enhances the endocytosis of K^d but also down-regulates K^d recycling.

Because K^d recycling was decreased by APLP2, we next ascertained whether K^d molecules were being transferred to the lysosomes. HeLa-etK^d cells that had been transfected with APLP2-FLAG for 24 h were labeled with the anti-K^d Ab 34-1-2 and incubated at 37 °C. After K^d uptake, non-internalized Abs were removed by acid wash, and the cells were subjected to a 4-h chase. The cells were then fixed and stained with anti-FLAG and anti-LAMP1 Abs for the transfected APLP2-FLAG and the LAMP1 lysosomal marker, respectively. Comparison of cells within the same fields that were transfected *versus*

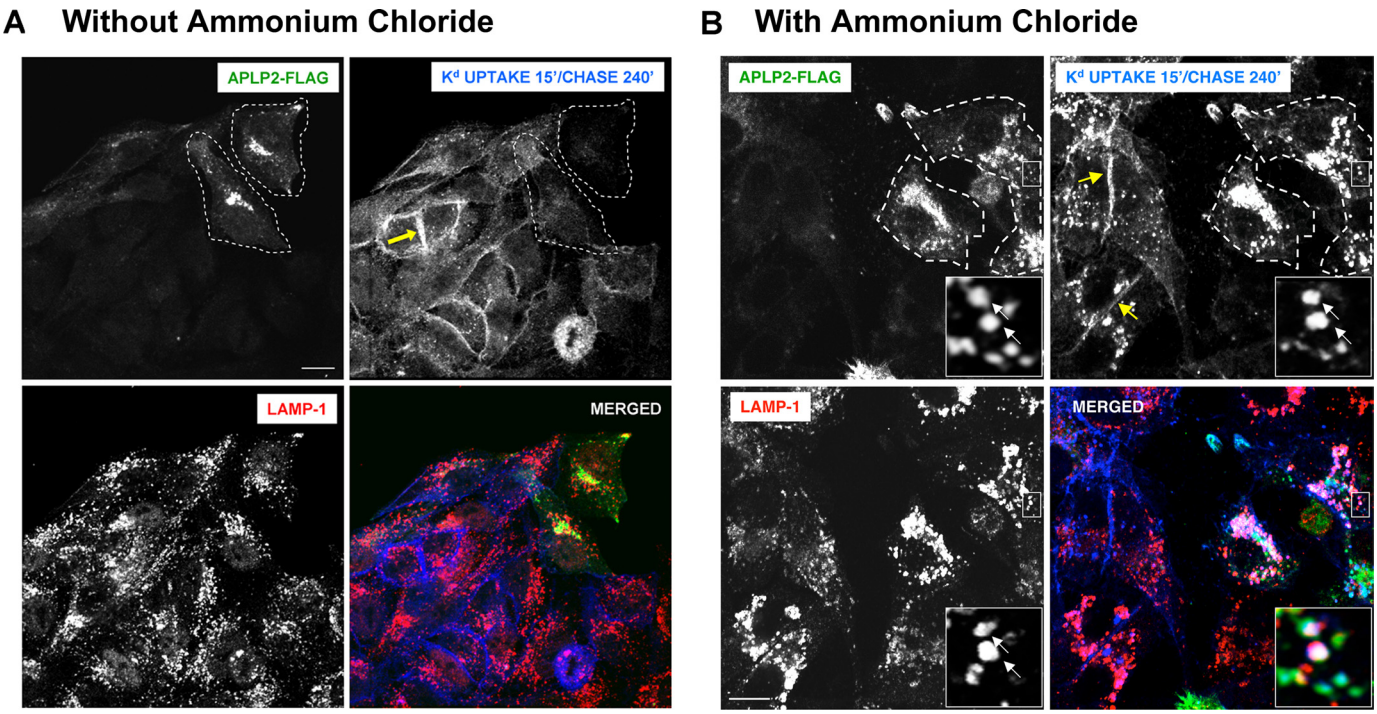

FIGURE 6. **K^d routing to lysosomes for degradation was increased in cells with a higher level of APLP2.** *A*, HeLa-etK^d cells transfected with APLP2-FLAG for 24 h were pulsed for 15 min at 37 °C with anti-K^d Ab 34-1-2. After the pulse, non-internalized cell surface-bound Abs were removed. The cells were transferred to complete medium for 4 h, and then fixed and stained with fluorescein isothiocyanate-conjugated goat anti-FLAG Ab and rabbit anti-LAMP1 Ab for 1 h. The cells were stained with Alexa Fluor 405 goat anti-mouse Ab (to identify the 34-1-2-labeled K^d molecules) and Alexa Fluor 568 goat anti-rabbit Ab (to identify the LAMP1 marker in the lysosomes). *Green*, APLP2-FLAG; *blue*, K^d; *red*, LAMP-1; *white*, co-localized APLP2-FLAG, K^d, and LAMP-1. *Bar*, 10 μm. *B*, the same procedure as in *A* was followed except that at 24 h the cells were treated with 20 mM ammonium chloride for 12 h before the 34-1-2 Ab pulse. The *insets* show a higher magnification of areas within the larger boxes, and the *arrows* point to representative lysosomes with co-localized APLP2-FLAG and K^d.

untransfected with APLP2-FLAG revealed that the cells that had been transfected with APLP2-FLAG (marked with a boundary line) had few or none of the 34-1-2 Ab-labeled K^d molecules still within the cells after the 4-h chase (Fig. 6*A*). With the cells that were not transfected with APLP2, most of the 34-1-2 Ab-labeled K^d molecules had recycled back to the plasma membrane (shown by an *arrow*) by 4 h (Fig. 6*A*).

To confirm the destination of the K^d molecules that were not being recycled to the plasma membrane, the cells were pre-treated with the lysosome inhibitor ammonium chloride at 24 h post-transfection with APLP2-FLAG. Ab 34-1-2 was added to bind to the cell surface K^d molecules, and the cells were warmed to cause K^d endocytosis. Remaining non-internalized Abs were stripped off by an acid wash, and the cells were incubated for a 4-h chase before they were stained with anti-FLAG and anti-LAMP1 Abs. In ammonium chloride-treated cells that were not APLP2-FLAG-transfected, by 4 h most of the labeled K^d molecules had recycled to the surface (Fig. 6*B*). Some intracellular vesicles in these non-APLP2-FLAG-transfected cells also contained labeled K^d molecules that may have been rescued from degradation due to the inhibition of lysosomal function (Fig. 6*B*). In contrast, in cells transfected with APLP2-FLAG and treated with ammonium chloride, internalized K^d molecules had accumulated in the lysosomes. This finding suggests that APLP2 had directed K^d molecules to the lysosomes, but because lysosomal function was blocked by ammonium chloride, the K^d molecules remained intact. Thus, in cells not treated with ammonium chloride, K^d trafficking to lysosomes and (as a consequence) its turnover in the lysosomes was increased upon elevation of the cellular level of APLP2.

DISCUSSION

Endocytosis of MHC class I molecules has been studied using several cell types as models, including lymphocytes, fibroblasts, and macrophages, with variability reported for the extent and pathway of internalization (35–46). The endocytosis of MHC class I molecules is dependent on a sequence in the MHC class I molecule cytoplasmic tail (40, 41, 47). Studies have indicated that MHC class I molecules are recycled to the cell surface after internalization (*e.g.* Ref. 42) by a process in which Eps15 homology domain-containing proteins (EHD1 and EHD4) play an important role (48–50). EHD1 causes the generation of tubules that contain endocytosed MHC class I molecules, and higher expression of EHD1 increases MHC class I recycling, whereas reduced EHD1 expression slows the rate of MHC class I recycling (48, 49).

In our studies, the endocytosis of K^d in HeLa-etK^d cells was not inhibited by dynamin II K44A or the C-terminal portion of AP180, indicating that endocytosis was primarily non-clathrin mediated. This observation with K^d is in agreement with previously published findings that the endocytosis of other MHC class I molecules occurs principally via a clathrin-independent path (35, 44), although there have also been reports that MHC class I molecules are internalized by a clathrin-dependent pathway in certain cell types (38, 39). Our observation that APLP2 can divert K^d into the clathrin-dependent pathway suggests

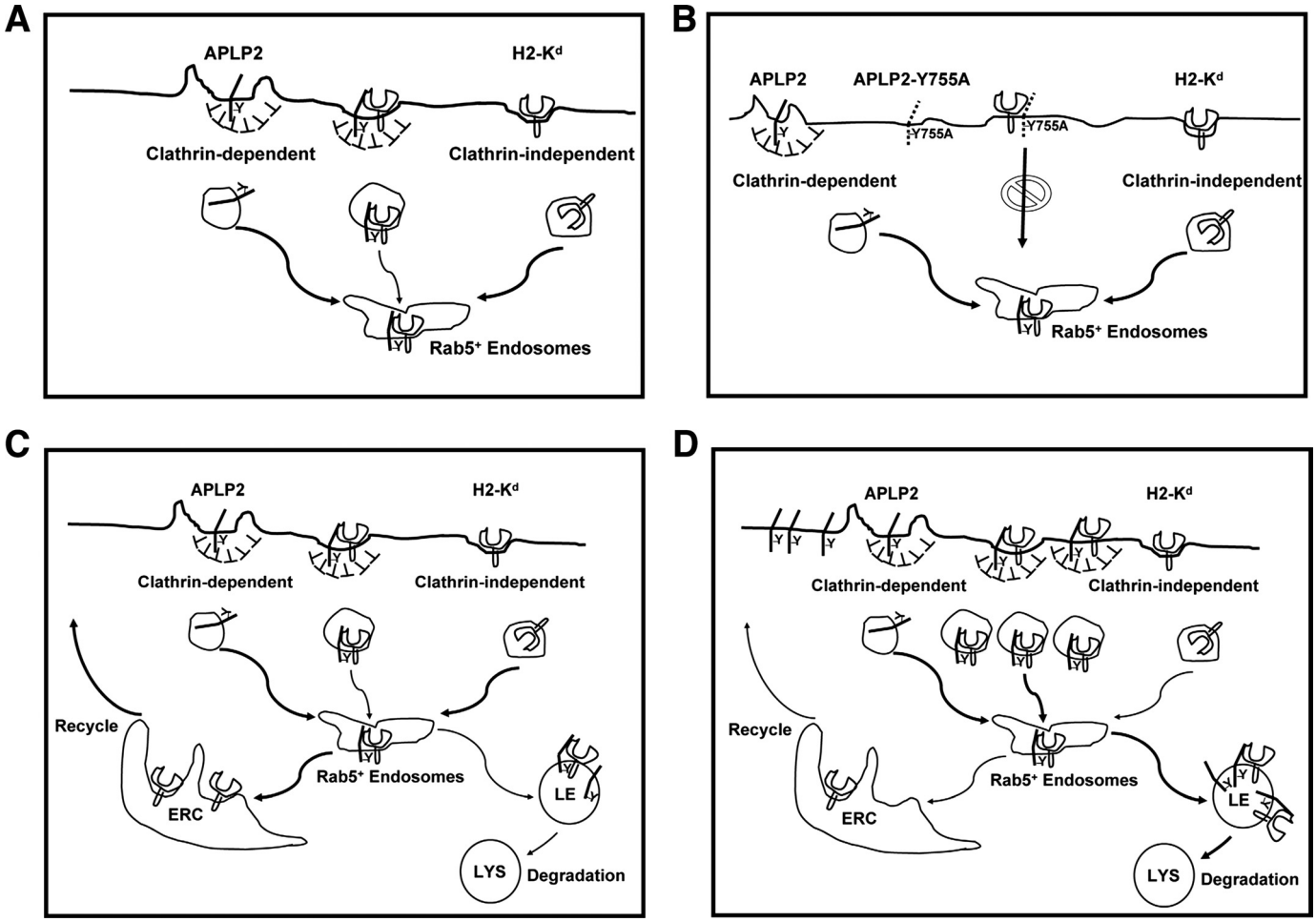

FIGURE 7. **Diagram of a model in which increased expression of APLP2 results in the recruitment of clathrin machinery at APLP2·K^d complexes, causing uptake of K^d in a clathrin-dependent manner and routing K^d to the lysosomes.** *A*, increased availability of APLP2 leads to more binding of APLP2 to K^d and subsequent internalization of both APLP2 and K^d by a clathrin-mediated mechanism into Rab5$^+$ early endosomes. *B*, inhibition of APLP2 clathrin-mediated endocytosis by mutation of Tyr-755 to alanine (as depicted) or by dynamin II K44A or the AP180 C-terminal fragment (not depicted in this figure) prevents APLP2 from enhancing K^d endocytosis. *C*, in cells with less APLP2, the majority of K^d molecules follow a recycling pathway from the Rab5$^+$ endosomes to the endocytic recycling compartment (*ERC*) and back to the cell surface (indicated by the *thick arrows*) and a minority traffic to late endosomes (*LE*) and lysosomes (*LYS*) (indicated by the *thin arrows*). *D*, in cells with a higher level of APLP2, the majority of K^d molecules follow a degradation pathway from the Rab5$^+$ endosomes to the lysosomes (*LYS*) (indicated by *thick arrows*), and a minority of K^d molecules enter a recycling pathway (indicated by *thin arrows*).

that the intervention of APLP2 or other non-MHC proteins in some cells may explain some of the differences in the pathways of MHC class I internalization that have been described.

Our findings showed that APLP2 endocytosis is dependent on the tyrosine at position 755, which is located within overlapping NP*X*Y and Y*XX*Ø motifs in the distal part of the APLP2 cytoplasmic domain. The Tyr-755 and both motifs are conserved between mouse and human APLP2. Furthermore, the signal for endocytosis of the closely related molecule APP has also been shown to rely on motifs in the cytoplasmic tail. The C-terminal domain of APP contains two overlapping NP*X*Y and Y*XX*Ø endocytic motifs within the sequence YENPTYKFF, and deletion of the YENPTY sequence in APP decreased APP endocytosis (51). Consistent with this finding, studies from several laboratories have shown that cells expressing either APP with the cytoplasmic domain deleted or APP mutated at the tyrosine in the NPTY cytoplasmic tail sequence secrete higher levels of soluble APP than cells expressing wild type APP, which could result from impairment of APP endocytosis (52–54). Subsequent mutational analysis defined the YENP sequence as the critical tetrapeptide motif for APP internalization and the tyrosine in the NPTY sequence as a lysosomal targeting signal for APP (55). Besides the dominant YENPTY sequence, the cytoplasmic tail of APP contains a YTSI sequence proximal to the transmembrane region that has another tyrosine-based endocytic motif (Y*XX*I). Mutation of the tyrosine in the YTSI sequence does not impair APP endocytosis, although this motif plays an important role in the basolateral targeting of APP in polarized cells (56).

In a previous study from our laboratories (4), APLP2 was discovered to interact with folded, internalized K^d molecules and facilitate K^d endocytosis. A study focused mainly on the closely related protein APP has been recently published (57), in which both APLP2 and APP were observed to interact with the high-affinity choline transporter, and APP was demonstrated to facilitate its endocytosis. Together, our findings and those of Wang *et al.* (57) suggest that APP family members APP and APLP2 play important roles in regulating expression of cell surface proteins. In our model of APLP2 regulation of K^d surface expression, APLP2 binds K^d at the plasma membrane (Fig. 7, *A* and *B*). Via the clathrin-mediated and AP-2-depen-

dent endocytosis (involving the Y755 in the APLP2 C terminus) of APLP2, APLP2 increases the internalization of K^d, diverting it away from its clathrin-independent route of endocytosis (Fig. 7, *A* and *B*). APLP2 increases the trafficking of the endocytosed K^d molecules to the late endocytic compartment and lysosomes, where the K^d molecules are degraded (Fig. 7, *C* and *D*). Thus, despite convergence at $Rab5^+$ early endosomes, the many K^d molecules escorted into the cell interior by APLP2 molecules as they take the clathrin pathway are principally destined for lysosomal destruction, whereas the fewer K^d molecules internalized via the clathrin-independent pathway when a lower level of APLP2 is expressed in the cell are predominantly recycled (Fig. 7, *C* and *D*).

APLP2 has been reported to be overexpressed in tumors (58), and APLP2 levels were noted to be higher in invasive breast cancer lesions than in non-invasive breast cancer lesions (59). Therefore, the effects of increased APLP2 on MHC class I molecules that we have demonstrated have possible implications not only in normal MHC class I molecule turnover but also in cancer evasion of the cellular immune response. Recent findings from our laboratory indicating that APLP2 is highly expressed in many human tumor cell lines and decreases the cell surface expression of human MHC class I molecules on tumor cells are consistent with this supposition (19). In addition, other functions of APLP2 related to cell signaling, adhesion, migration, and proliferation, which may play a role both in normal cell physiology and in malignancy, may all be influenced, directly or indirectly, by the endocytosis of APLP2. Overall, our analyses of APLP2-directed endocytosis of MHC class I molecules provide significant new perspectives on crucial cellular processes.

Acknowledgments—We are grateful to Dr. W. Maury and Dr. T. Hansen for donations of Abs and cell lines, and Drs. M. McNiven, J. Donaldson, L. Greene, and R. Lodge for DNA constructs. We also thank the personnel of the UNMC Monoclonal Antibody Facility and the University of Nebraska Center for Biotechnology for assistance. Core facilities at the University of Nebraska Medical Center receive support from National Institutes of Health NCI Cancer Center Support Grant P30CA036727 (to the Eppley Cancer Center) and the Nebraska Research Initiative.

REFERENCES

1. Feuerbach, D., and Burgert, H. G. (1993) *EMBO J.* **12,** 3153–3161
2. Sester, M., Feuerbach, D., Frank, R., Preckel, T., Gutermann, A., and Burgert, H. G. (2000) *J. Biol. Chem.* **275,** 3645–3654
3. Morris, C. R., Petersen, J. L., Vargas, S. E., Turnquist, H. R., McIlhaney, M. M., Sanderson, S. D., Bruder, J. T., Yu, Y. Y., Burgert, H. G., and Solheim, J. C. (2003) *J. Biol. Chem.* **278,** 12618–12623
4. Tuli, A., Sharma, M., McIlhaney, M. M., Talmadge, J. E., Naslavsky, N., Caplan, S., and Solheim, J. C. (2008) *J. Immunol.* **181,** 1978–1987
5. Wolfe, M. S., and Guénette, S. Y. (2007) *J. Cell Sci.* **120,** 3157–3161
6. Zheng, H., and Koo, E. H. (2006) *Mol. Neurodegener.* **1,** 5
7. Lo, A. C., Thinakaran, G., Slunt, H. H., and Sisodia, S. S. (1995) *J. Biol. Chem.* **270,** 12641–12645
8. Slunt, H. H., Thinakaran, G., Von Koch, C., Lo, A. C., Tanzi, R. E., and Sisodia, S. S. (1994) *J. Biol. Chem.* **269,** 2637–2644
9. Thinakaran, G., Kitt, C. A., Roskams, A. J., Slunt, H. H., Masliah, E., von Koch, C., Ginsberg, S. D., Ronnett, G. V., Reed, R. R., and Price, D. L. (1995) *J. Neurosci.* **15,** 6314–6326
10. Rassoulzadegan, M., Yang, Y., and Cuzin, F. (1998) *EMBO J.* **17,** 4647–4656
11. Guo, J., Thinakaran, G., Guo, Y., Sisodia, S. S., and Yu, F. X. (1998) *Invest. Ophthalmol. Vis. Sci.* **39,** 292–300
12. Cappai, R., Mok, S. S., Galatis, D., Tucker, D. F., Henry, A., Beyreuther, K., Small, D. H., and Masters, C. L. (1999) *FEBS Lett.* **442,** 95–98
13. Li, X. F., Thinakaran, G., Sisodia, S. S., and Yu, F. S. (1999) *J. Biol. Chem.* **274,** 27249–27256
14. Scheinfeld, M. H., Ghersi, E., Laky, K., Fowlkes, B. J., and D'Adamio, L. (2002) *J. Biol. Chem.* **277,** 44195–44201
15. Walsh, D. M., Fadeeva, J. V., LaVoie, M. J., Paliga, K., Eggert, S., Kimberly, W. T., Wasco, W., and Selkoe, D. J. (2003) *Biochemistry* **42,** 6664–6673
16. Kaether, C., Schmitt, S., Willem, M., and Haass, C. (2006) *Traffic* **7,** 408–415
17. Rajendran, L., Honsho, M., Zahn, T. R., Keller, P., Geiger, K. D., Verkade, P., and Simons, K. (2006) *Proc. Natl. Acad. Sci. U.S.A.* **103,** 11172–11177
18. Tuli, A., Sharma, M., Naslavsky, N., Caplan, S., and Solheim, J. C. (2008) *Immunogenetics* **60,** 303–313
19. Tuli, A., Sharma, M., Wang, X., Simone, L. C., Capek, H. L., Cate, S., Hildebrand, W. H., Naslavsky, N., Caplan, S., and Solheim, J. C. (2009) *Cancer Immunol. Immunother.* **58,** 1419–1431
20. Damke, H., Baba, T., Warnock, D. E., and Schmid, S. L. (1994) *J. Cell Biol.* **127,** 915–934
21. Zhao, X., Greener, T., Al-Hasani, H., Cushman, S. W., Eisenberg, E., and Greene, L. E. (2001) *J. Cell Sci.* **114,** 353–365
22. Boll, W., Rapoport, I., Brunner, C., Modis, Y., Prehn, S., and Kirchhausen, T. (2002) *Traffic* **3,** 590–600
23. Bonifacino, J. S., and Traub, L. M. (2003) *Annu. Rev. Biochem.* **72,** 395–447
24. Ozato, K., Evans, G. A., Shykind, B., Margulies, D. H., and Seidman, J. G. (1983) *Proc. Natl. Acad. Sci. U.S.A.* **80,** 2040–2043
25. Smith, J. D., Myers, N. B., Gorka, J., and Hansen, T. H. (1993) *J. Exp. Med.* **178,** 2035–2046
26. Yu, Y. Y., Myers, N. B., Hilbert, C. M., Harris, M. R., Balendiran, G. K., and Hansen, T. H. (1999) *Int. Immunol.* **11,** 1897–1906
27. Myers, N. B., Harris, M. R., Connolly, J. M., Lybarger, L., Yu, Y. Y., and Hansen, T. H. (2000) *J. Immunol.* **165,** 5656–5663
28. Harris, M. R., Lybarger, L., Myers, N. B., Hilbert, C., Solheim, J. C., Hansen, T. H., and Yu, Y. Y. (2001) *Int. Immunol.* **13,** 1275–1282
29. Lybarger, L., Yu, Y. Y., Chun, T., Wang, C. R., Grandea, A. G., 3rd, Van Kaer, L., and Hansen, T. H. (2001) *J. Immunol.* **167,** 2097–2105
30. Stenmark, H., Parton, R. G., Steele-Mortimer, O., Lütcke, A., Gruenberg, J., and Zerial, M. (1994) *EMBO J.* **13,** 1287–1296
31. Turnquist, H. R., and Solheim, J. C. (2001) *Methods Mol. Biol.* **156,** 165–173
32. Traub, L. M. (2003) *J. Cell Biol.* **163,** 203–208
33. Keyel, P. A., Mishra, S. K., Roth, R., Heuser, J. E., Watkins, S. C., and Traub, L. M. (2006) *Mol. Biol. Cell* **17,** 4300–4317
34. Maurer, M. E., and Cooper, J. A. (2006) *J. Cell Sci.* **119,** 4235–4246
35. Huet, C., Ash, J. F., and Singer, S. J. (1980) *Cell* **21,** 429–438
36. Tse, D. B., and Pernis, B. (1984) *J. Exp. Med.* **159,** 193–207
37. Machy, P., Barbet, J., and Leserman, L. D. (1982) *Proc. Natl. Acad. Sci. U.S.A.* **79,** 4148–4152
38. Machy, P., Truneh, A., Gennaro, D., and Hoffstein, S. (1987) *Nature* **328,** 724–726
39. Dasgupta, J. D., Watkins, S., Slayter, H., and Yunis, E. J. (1988) *J. Immunol.* **141,** 2577–2580
40. Capps, G. G., Van Kampen, M., Ward, C. L., and Zúñiga, M. C. (1989) *J. Cell Biol.* **108,** 1317–1329
41. Vega, M. A., and Strominger, J. L. (1989) *Proc. Natl. Acad. Sci. U.S.A.* **86,** 2688–2692
42. Reid, P. A., and Watts, C. (1990) *Nature* **346,** 655–657
43. Hochman, J. H., Jiang, H., Matyus, L., Edidin, M., and Pernis, B. (1991) *J. Immunol.* **146,** 1862–1867
44. Radhakrishna, H., and Donaldson, J. G. (1997) *J. Cell Biol.* **139,** 49–61
45. Chiu, I., Davis, D. M., and Strominger, J. L. (1999) *Proc. Natl. Acad. Sci. U.S.A.* **96,** 13944–13949
46. Grommé, M., Uytdehaag, F. G., Janssen, H., Calafat, J., van Binnendijk, R. S., Kenter, M. J., Tulp, A., Verwoerd, D., and Neefjes, J. (1999) *Proc. Natl.*

Acad. Sci. U.S.A. **96,** 10326–10331
47. Santos, S. G., Antoniou, A. N., Sampaio, P., Powis, S. J., and Arosa, F. A. (2006) *J. Immunol.* **176,** 2942–2949
48. Caplan, S., Naslavsky, N., Hartnell, L. M., Lodge, R., Polishchuk, R. S., Donaldson, J. G., and Bonifacino, J. S. (2002) *EMBO J.* **21,** 2557–2567
49. Naslavsky, N., Boehm, M., Backlund, P. S., Jr., and Caplan, S. (2004) *Mol. Biol. Cell* **15,** 2410–2422
50. Sharma, M., Naslavsky, N., and Caplan, S. (2008) *Traffic* **9,** 995–1018
51. Lai, A., Sisodia, S. S., and Trowbridge, I. S. (1995) *J. Biol. Chem.* **270,** 3565–3573
52. Haass, C., Hung, A. Y., Schlossmacher, M. G., Teplow, D. B., and Selkoe, D. J. (1993) *J. Biol. Chem.* **268,** 3021–3024
53. De Strooper, B., Umans, L., Van Leuven, F., and Van Den Berghe, H. (1993) *J. Cell Biol.* **121,** 295–304
54. Jacobsen, J. S., Spruyt, M. A., Brown, A. M., Sahasrabudhe, S. R., Blume, A. J., Vitek, M. P., Muenkel, H. A., and Sonnenberg-Reines, J. (1994) *J. Biol. Chem.* **269,** 8376–8382
55. Perez, R. G., Soriano, S., Hayes, J. D., Ostaszewski, B., Xia, W., Selkoe, D. J., Chen, X., Stokin, G. B., and Koo, E. H. (1999) *J. Biol. Chem.* **274,** 18851–18856
56. Lai, A., Gibson, A., Hopkins, C. R., and Trowbridge, I. S. (1998) *J. Biol. Chem.* **273,** 3732–3739
57. Wang, B., Yang, L., Wang, Z., and Zheng, H. (2007) *Proc. Natl. Acad. Sci. U.S.A.* **104,** 14140–14145
58. Covell, D. G., Wallqvist, A., Rabow, A. A., and Thanki, N. (2003) *Mol. Cancer Ther.* **2,** 317–332
59. Abba, M. C., Drake, J. A., Hawkins, K. A., Hu, Y., Sun, H., Notcovich, C., Gaddis, S., Sahin, A., Baggerly, K., and Aldaz, C. M. (2004) *Breast Cancer Res.* **6,** R499–513